Dual spin filter effect in a zigzag graphene nanoribbon

Taisuke Ozaki,[1] Kengo Nishio,[2] Hongming Weng,[1] and Hiori Kino[3]
[1]*Research Center for Integrated Science (RCIS), Japan Advanced Institute of Science and Technology (JAIST), 1-1 Asahidai, Nomi, Ishikawa 923-1292, Japan*
[2]*Research Institute for Computational Sciences (RICS), National Institute of Advanced Industrial Science and Technology (AIST), 1-1-1 Umezono, Tsukuba, Ibaraki 305-8568, Japan*
[3]*National Institute for Material Science (NIMS), 1-2-1 Sengen, Tsukuba, Ibaraki 305-0047, Japan*
(Received 30 April 2009; revised manuscript received 18 December 2009; published 17 February 2010)

By first principle calculations, a dual spin filter effect under finite bias voltages is demonstrated in an antiferromagnetic junction of symmetric zigzag graphene nanoribbon (ZGNR). Unlike conventional spin filter devices using half metallic materials, the up and down-spin electrons are unidirectionally filtered in the counter direction of the bias voltage, making the junction a dual spin filter. On the contrary, asymmetric ZGNRs do not exhibit such a spin filter effect. By analyzing Wannier functions and a tight-binding model, we clarify that an interplay between the spin polarized band structure of π and π^* states near the Fermi level and decoupling of the interband hopping of the two states, arising from the symmetry of the wave functions, plays a crucial role in the effect.

DOI: 10.1103/PhysRevB.81.075422 PACS number(s): 85.75.−d, 71.15.−m, 72.25.−b, 73.63.−b

I. INTRODUCTION

The graphenes have been recently attracting much attention as a candidate material for spintronics devices because of its peculiar electronic structures,[1–7] while so far most of promising materials in developing the devices have been found in ferromagnetic (FM) metals and FM semiconductors such as GaMnAs.[8] In fact, recent experiments have achieved spin injection into graphene layers at room temperature for the first time among molecular materials[1,2] and observed the magnetoresistance (MR) effect.[2] In addition, several intriguing transport properties have been theoretically predicted especially for zigzag graphene nanoribbons (ZGNRs).[3–7,9–13] For instance, it is shown that ZGNRs can be utilized even for generation of a spin polarized current, in which an external electric field applied across ZGNR along the lateral direction may induce a half-metallic band structure being responsible for the spin polarized current.[3] Also an extraordinary large MR and generation of spin-polarized current are also theoretically found in a spin valve device consisting of ZGNR.[5] The unique properties in the electronic transport properties of ZGNRs can be attributed to the characteristic band structures of ZGNR and the symmetry of wave functions near the Fermi level.[3–5] Along this line, the family of graphenes related to ZGNR might be anticipated to exhibit unexpected electronic properties which can be useful in developing spintronics devices. However, transport properties of ZGNRs under *finite* source-drain bias voltages V_{bias} have not been fully explored even from the theoretical points of view. For development of future device applications it is highly important to fully understand intrinsic behaviors in the transport properties of ZGNRs under a wide range of finite bias voltages.

In this paper, we present a unique and intrinsic electronic transport property of ZGNR under finite bias voltage V_{bias}, based on first principle calculations, that a symmetric ZGNR with an antiferromagnetic (AFM) junction exhibits a dual spin filter effect under finite V_{bias}, namely, the up and down-spin electrons are unidirectionally filtered in the counter direction of V_{bias}. Based on an analysis using Wannier functions (WFs) and a tight-binding (TB) model, we further clarify that the spin filter effect arises from an interplay between the band structure and absence of the interband hopping of the π and π^* states near the Fermi level.

II. COMPUTATIONAL DETAILS

At each bias voltage V_{bias} the electronic structure of ZGNR shown in Fig. 1(a) is self-consistently determined under an electronic temperature of 300 K by means of a nonequilibrium Green's function (NEGF) method[14,15] coupled with a local spin density approximation (LSDA) (Ref. 16) in the density-functional theory (DFT).[17] The equilibrium density matrix (DM) is evaluated by a contour integration method,[18] while the nonequilibrium DM is numerically computed on a line with an imaginary part of 0.01 eV, which is parallel to real axis in complex plane.[19] The conductance and current are calculated by the Landauer formula.[20] Norm-conserving pseudopotentials are used in a separable form with multiple projectors to replace the deep core potential into a shallow potential.[21] Pseudoatomic orbitals (PAOs) centered on atomic sites are used as basis functions. The PAO basis functions, generated by a confinement scheme,[22] are specified by H5.5-*s*2 and C4.5-*s*2*p*2, where the abbreviation of basis functions, such as C4.5-*s*2*p*2, represents that C stands for the atomic symbol, 4.5 the cutoff radius (Bohr) in the generation by the confinement scheme,[22] and *s*2*p*2 means the employment of two primitive orbital for each of *s* and *p* orbitals. The real space grid techniques are used with the energy cutoff of 120 Ry as a required cutoff energy in numerical integrations and the solution of Poisson equation using fast fourier transform (FFT).[23] In addition, the projector expansion method is employed in the calculation of three-center integrals for the deep neutral atom potentials.[24] The geometrical structures used are optimized with a criterion of 10^{-4} hartree/bohr for forces on atoms under the periodic boundary condition. All the calculations were performed by

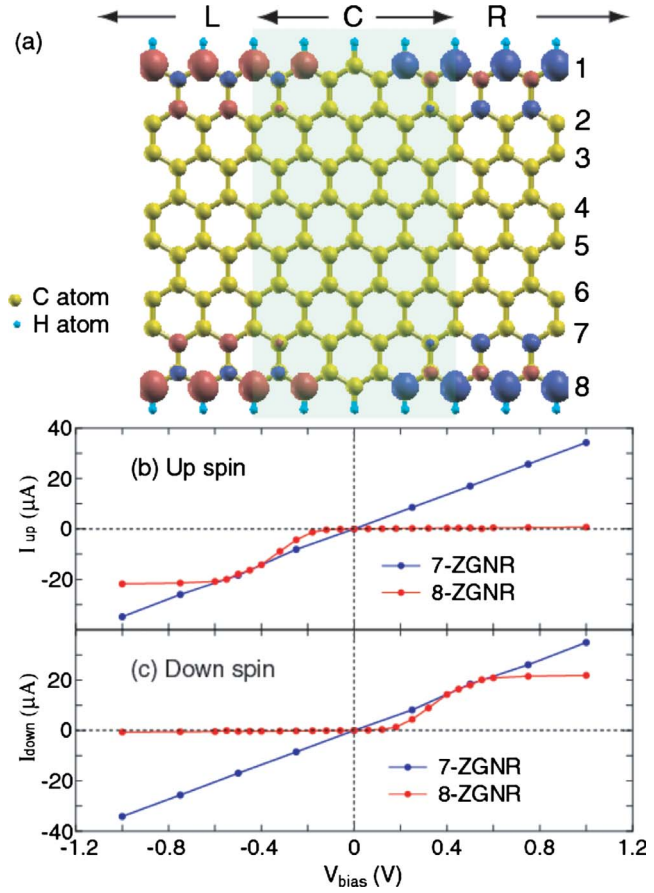

FIG. 1. (Color online) (a) 8-ZGNR, terminated by hydrogen atoms, with an AFM junction together with the spatial distribution of the spin density at $V_{bias}=0$ V, where the red and blue colors stands for positive and negative signs, and *L*, *R*, and *C* means the *left* and *right* leads, and the *central* scattering region of which lengths are 4.88, 4.88, and 9.76 Å, respectively, and width is 17.78 Å. *I*-V_{bias} curves for (b) the up-spin and (c) the down-spin states of seven and 8-ZGNRs with the AFM junction.

an *ab initio* DFT code, OPENMX.[25]

III. RESULTS

n-ZGNRs are characterized by the number of carbon atoms, even (symmetric) or odd (antisymmetric), in the sublattice being across ZGNR along the lateral direction, while Fig. 1(a) shows the case of eight carbon atoms abbreviated as 8-ZGNR. For ZGNRs we focus a spin configuration with an AFM junction as shown in Fig. 1(a). Considerable magnetic moments are found at both the zigzag edges which can be attributed to the existence of the flat band near *X* point.[26] Although the AFM coupling between the zigzag edges is favored by about 10 meV per edge carbon atom compared to the FM coupling, we consider the spin configuration consisting of the FM coupling between the zigzag edges and the AFM junction at the central region. The spin configuration is crucial for the spin filter effect we discuss, and might be realized by a magnetic field applied in a spin valve device or chemical modifications for ZGNRs. It should be noted that

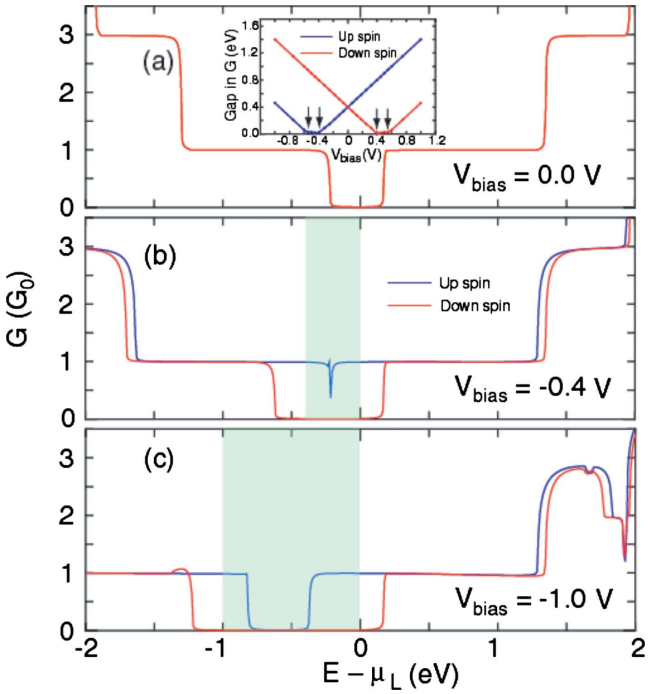

FIG. 2. (Color online) Conductance of 8-ZGNR with the AFM junction with V_{bias} of (a) 0.0, (b) −0.4, and (c) −1.0 V. The inset in (a) shows the conductance gap near the chemical potentials.

the effect does not appear in the other spin configurations.[27] The current-voltage (*I*-*V*) characteristics for 8-ZGNR with the spin configuration depends on intriguingly not only spin, but also the direction of V_{bias} as shown in Figs. 1(b) and 1(c). Interestingly, the up-spin electron substantially flows only in the negative regime of V_{bias}, while the down-spin electron flows only in the positive regime. The ratio of the spin dependent currents, I_{up}/I_{down}, turns out to be 44.3 at −0.4 V, and the value is equivalent to the rectification ratio for each spin-dependent current because of the *I*-*V* characteristics. The *I*-*V* characteristics of other even cases, $n=6$ and 10, are also found to be nearly equivalent. Thus, a symmetric ZGNR plays *dual* roles as a unidirectional spin filter for *each* spin state under finite V_{bias}. The effect can also be regarded as a dual spin *diode* effect due to the unidirectional nature of the spin-dependent current. In contrast, the current for 7-ZGNR with the spin configuration is almost independent of spin, and proportional to V_{bias} within the regime, leading to I_{up}/I_{down} of a nearly one. Thus, it should be emphasized that the parity in the geometrical structure of *n*-ZGNR is the key factor even for the behavior of the spin polarized current as in the spin unpolarized current.[4]

The *I*-*V* characteristics for 8-ZGNR is understood by examining the dependency of the conductance on V_{bias}. It is found in Fig. 2(a) that there is a conductance gap of about 0.4 eV for both the up and down-spin states around the chemical potential at $V_{bias}=0$ V. The gap for the up-spin state decreases as V_{bias} increases toward the negative direction, and approaches zero at about $V_{bias}=-0.4$ V as shown in Fig. 2(b), while the zero gap is kept up to $V_{bias}=-0.55$ V. From then onwards the gap increases as illustrated in Fig. 2(c). On the other hand, the gap for the down-spin state

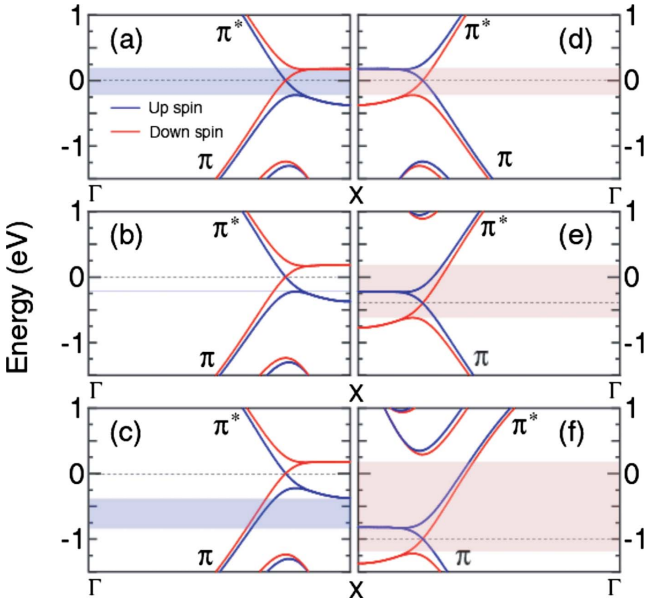

FIG. 3. (Color online) (a)–(c) Band structures of 8-ZGNR with a FM coupling corresponding to the *left* lead region in Fig. 1(a). Band structures shifted with (d) 0.0, (e) −0.4, and (f) −1.0 eV of 8-ZGNR with a FM coupling corresponding to the *right* lead region in Fig. 1(a), where the roles of the up and down-spin states are reversed because of the opposite spin direction in the right lead. The blue and red shades show the conductance gap for the up and down-spin electrons, respectively. The horizontal dot line indicates the chemical potential, being position dependent, of 8-ZGNR shown in Fig. 1(a).

monotonically increases as V_{bias} increases toward the negative direction. The conductance gaps for the up and down-spin states are shown as a function of V_{bias} in the inset of Fig. 2(a). We see that the behavior of the gaps is opposite for the up and down-spin states in the regime of the positive direction of V_{bias} in contrast with that in the negative direction. The shaded regions in Figs. 2(b) and 2(c) correspond to the regime in between two chemical potentials of the left and right leads, where the electron transmission can contribute to the current flow. Thus, it is confirmed that in the regime of the negative V_{bias}, $|I_{\text{up}}|$ increases up to around $V_{\text{bias}}=-0.55$ V, where the gap opening occurs again, and from then onwards saturated. Also it turns out that $|I_{\text{down}}|$ should be nearly zero in the regime of the negative V_{bias}, since the shaded region is always inlying in the conductance gap for the down-spin state. In the regime of the positive V_{bias}, the *I-V* characteristics can be explained in the same way by considering the reversed roles of up and down-spin states. Note that the reversal of the roles arises only in the spin configuration with the AFM junction.

The opening and closing of the conductance gap can be attributed to the band structure near the Fermi level of 8-ZGNR with the FM coupling between the zigzag edges. The exchange splitting Δ_x is found to be 0.553 eV at *X* point from Fig. 3(a). The right blue and pink shades denote the conductance gaps for the up and down-spin states in Fig. 2. It is clearly seen that the conductance gap corresponds to an energy regime where the $\pi(\pi^*)$ state in the left panel overlaps with *only* the $\pi^*(\pi)$ state with the same spin in the corresponding right panel. The π^* up-spin state in Fig. 3(a) overlaps with *only* the π up-spin state in Fig. 3(d) in the conductance gap. Once the overlap regime fades away at the situation given by Figs. 3(b) and 3(e), and then onward it turns out that the π up-spin state in Fig. 3(c) overlaps with *only* the π^* up-spin state in Fig. 3(f) in the regime of the conductance gap. On the other hand, for the down-spin state the energy regime, where the π state in the left panel overlaps with *only* the π^* state in the right panel, linearly increases as the energy shift increases toward the negative direction as shown in Figs. 3(d)–3(f). The same idea except for reversing of the roles of the π and π^* states can apply to the case of the energy shift toward the positive direction. Since the band structures in the left and right panels can be regarded as those of the left and right leads in Fig. 1(a), the correspondence implies that the electron transmission from the $\pi(\pi^*)$ to $\pi^*(\pi)$ states is forbidden. In fact, it is shown that the Bloch function of the π (π^*) state is antisymmetric (symmetric) with respect to the σ mirror plane which is the mid plane between two edges.[4,5] Thus, the electron transmission should be forbidden in the energy regime where the π (π^*) overlaps with *only* the π^* (π) states. The band structure of 7-ZGNR with the FM coupling between the zigzag edges is very similar to that of 8-ZGNR so that the above analysis can also apply to the case. However, as discussed later the transmission is allowed even for the energy regime, where *only* the overlap between the π (π^*) and the π^* (π) states survives, due to the absence of the mirror plane in 7-ZGNR, leading to the linear *I-V* characteristics as shown in Figs. 1(b) and 1(c).

To further verify the physical origin, explained above, of the peculiar *I-V* curves which can be determined by the characteristic band structure of ZGNRs and the symmetry of wave functions, we construct WFs for the π and π^* states for 7- and 8-ZGNRs with the nonmagnetic state by the method of constructing maximally localized generalized Wannier functions.[28,29] In the generation of WFs the outer energy window from −3 to 3 eV and the inner energy window from −1.2 to 1.2 eV are used so that the two bands of π and π^* states are included, and two bands corresponding to π and π^* states are selected by the disentangling process.[28] In addition, extended states spreading over the central unit cell are used as the initial guess. The treatment enables us to obtain a physically appealing *molecular* orbital rather than *atomic* orbital as WF, which can be regarded as an envelope wave function. As a result, the obtained WFs are not maximally localized WFs, but correspond to local minima of the spread functional. Those of 8-ZGNR are shown in Figs. 4(a) and 4(b). We also evaluate TB parameters using WFs for our TB Hamiltonian of the even ZGNRs given by $H=\Sigma(\varepsilon_\mu + \delta_{ss_0}\Delta_x)c^\dagger_{\mu is}c_{\mu is}+\Sigma_{i\neq j}h_{\mu\mu,|i-j|}c^\dagger_{\mu is}c_{\mu js}$, where μ is the band index for the π and π^* states, i and j are site indices along the horizontal direction in Fig. 4(a) or Fig. 4(b), and s is the spin index. Also, δ is the Kronecker delta and s_0 is $\downarrow$ and $\uparrow$ in the left and right lead regions, respectively. It is confirmed that WFs of 7-ZGNR is neither symmetric nor antisymmetric (not shown), and that the absolute value of the nearest-neighbor hopping integral $h_{\pi\pi^*,1}$ between the π and π^* states is 0.485 eV, which is comparable to the nearest neighbor hopping integral $h_{\pi\pi,1}$ ($h_{\pi^*\pi^*,1}$) for the π (π^*) state of −0.777

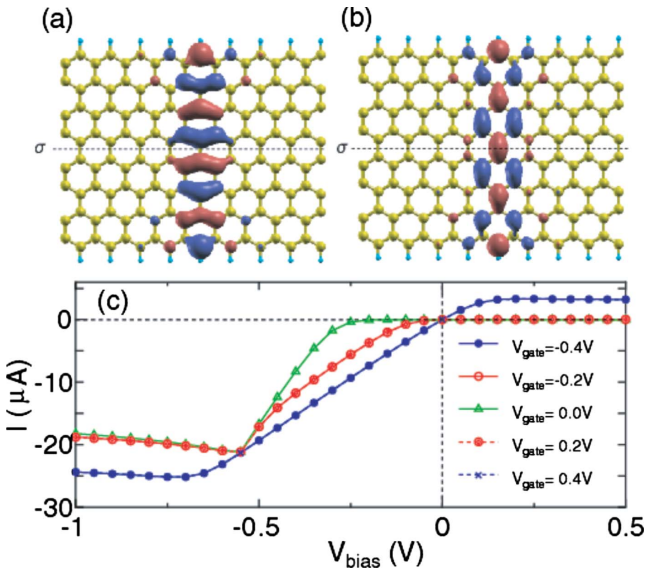

FIG. 4. (Color online) Wannier functions for (a) the π and (b) π^* states of the nonspin polarized 8-ZGNR. (c) I-V_{bias} curves of the up-spin state calculated by the simple TB model with the AFM junction for a series of the gate voltage V_{gate}.

(0.784) eV, where the nearest-neighbor hopping integral is defined by the integral between two relevant WFs centered at the central cell and the nearest neighboring cell, respectively. On the other hand, WFs for the π and π^* states of 8- ZGNR are antisymmetric and symmetric with respect to the σ mirror plane, and localized in three unit cells along the ribbon direction as shown in Figs. 4(a) and 4(b). We confirm that the hopping integrals $h_{\pi\pi^*,n}$ between WFs for the π and π^* states are nearly zero (not shown). Also it turns out that the next nearest neighbor hopping integral and more $|h_{\mu\mu,n}|(n=2-4)$ between the π (π^*) states centered at different unit cells are one order smaller than $|h_{\mu\mu,1}|$ as shown in Table I. Thus, we can construct a simple TB model determined by a fitting, containing the essence of the spin filter effect, which consists of only the on-site energy, the nearest-neighbor hopping integral, and the exchange splitting Δ_x. The fitted parameters in Table I are determined so that the bandwidth and the degeneracy of the π and π^* states at X point can be reproduced. It should be noted that the two band TB model can be decomposed into two decoupled one band models due to the decoupling of the π and π^* states. The fact allows us to evaluate a spin polarized current for the $\pi(\pi^*)$ state using the Landauer formula[20] for the one band TB model and the fitted parameters as

$$I = \int dE(f_L - f_R)T(E), \tag{1}$$

where f_L and f_R are the Fermi functions with the chemical potentials for the left and right leads, respectively. The transmission T is given by an analytic formula,

$$T(E) = \frac{4S_L(E)S_R(E)}{[S_L(E) + S_R(E)]^2}, \tag{2}$$

with

$$S_L(E) = \sqrt{4h_1^2 - \left[E - \left(\varepsilon - \frac{1}{2}\Delta_x\right)\right]^2}, \tag{3}$$

$$S_R(E) = \sqrt{4h_1^2 - \left[E - \left(\varepsilon + \frac{1}{2}\Delta_x + V_{\text{bias}}\right)\right]^2}, \tag{4}$$

where S_L and S_R are not zero only if the number in the square root is larger than zero, and therefore the transmission is finite within the energy range where both S_L and S_R survive. It is emphasized that the behaviors of the conductance gap in Fig. 2 can be easily traced by the model. Using Eq. (1) we evaluate the gate voltage dependency of the I-V characteristics for the up-spin state as shown in Fig. 4(c), where Δ_x of 0.553 eV, being that of the spin polarized 8-ZGNR, is used, and the gate voltage V_{gate} is taken into account by adding V_{gate} to the on-site energy. The proposed TB model can be validated by the fact that the I-V characteristics at $V_{\text{gate}}=0.0$ V is quite similar to that in Fig. 1(b) calculated by the NEGF method. In addition, it is found that the I-V characteristics does not largely change as long as V_{gate} lies in between $\pm\frac{1}{2}\Delta_x$, while the absolute threshold voltage at which the current starts to flow can be tuned. However, once $|V_{\text{gate}}|$ exceeds $\frac{1}{2}\Delta_x$, the originally suppressed current starts to leak in the positive V_{bias} regime. The leak current is due to the fact that one of the chemical potentials is located at the outside of the conductance gap. In case that ZGNR contacts with a metallic substrate, the Fermi level of ZGNR might be shifted by charge transfer between them. For such a case the gate voltage dependency apparently suggests that the Fermi levels must be adjusted within the energy regime of the exchange splitting by applying a proper gate voltage in order to keep the high $I_{\text{up}}/I_{\text{down}}$.

TABLE I. Tight-binding parameters (eV) evaluated by WFs denoted by *WF*, and a fitting, denoted by *fitted*, for the π and π^* states of the nonspin polarized 8-ZGNR, where ε_μ is the on-site energy, and $h_{\mu\mu,1}$, $h_{\mu\mu,2}\cdots$ the nearest and the second nearest-neighbor hopping integrals, and so on, and μ is either π or π^*. The Fermi level is set to zero.

μ	ε_μ	$h_{\mu\mu,1}$	$h_{\mu\mu,2}$	$h_{\mu\mu,3}$	$h_{\mu\mu,4}$
π (WF)	−1.3609	−0.7660	0.0076	0.0529	−0.0352
π^* (WF)	1.4486	0.7708	−0.0400	−0.0513	0.0269
π (fitted)	−1.4165	−0.7083	0	0	0
π^* (fitted)	1.4135	0.7067	0	0	0

IV. CONCLUSIONS

In summary, we demonstrate based on the NEGF method coupled with DFT that the symmetric ZGNRs with an AFM junction possess intrinsically a peculiar *I-V* characteristics, which can be regarded as a dual spin filter effect. It is shown by analyzing the band structure, WFs of the π and π^* states, and a TB model that the physical origin of the spin filter effect can be attributed to the spin polarized band structure of the symmetric ZGNR and the symmetry of wave functions of the π and π^* states near the Fermi level. The dual spin filter effect might initiate a novel avenue in developing spintronics using graphene based devices.

ACKNOWLEDGMENTS

This work is partly supported by CREST-JST, the Next Generation Supercomputing Project, Nanoscience Program, and NEDO (as part of the Nanoelectronics project).

[1] M. Ohishi, M. Shiraishi, R. Nouchi, T. Nozaki, T. Shinjo, and Y. Suzuki, Jpn. J. Appl. Phys. **46**, L605 (2007).
[2] N. Tombros, C. Jozsa, M. Popinciuc, H. T. Jonkman, and B. J. van Wees, Nature (London) **448**, 571 (2007).
[3] Y.-W. Son, M. L. Cohen, and S. G. Louie, Nature (London) **444**, 347 (2006).
[4] Z. Li, H. Qian, J. Wu, B.-L. Gu, and W. Duan, Phys. Rev. Lett. **100**, 206802 (2008).
[5] W. Y. Kim and K. S. Kim, Nat. Nanotechnol. **3**, 408 (2008).
[6] D. A. Abanin, P. A. Lee, and L. S. Levitov, Phys. Rev. Lett. **96**, 176803 (2006).
[7] O. V. Yazyev and M. I. Katsnelson, Phys. Rev. Lett. **100**, 047209 (2008).
[8] I. Zutic, J. Fabian, and S. D. Sarma, Rev. Mod. Phys. **76**, 323 (2004).
[9] V. M. Karpan, G. Giovannetti, P. A. Khomyakov, M. Talanana, A. A. Starikov, M. Zwierzycki, J. van den Brink, G. Brocks, and P. J. Kelly, Phys. Rev. Lett. **99**, 176602 (2007).
[10] V. M. Karpan, P. A. Khomyakov, A. A. Starikov, G. Giovannetti, M. Zwierzycki, M. Talanana, G. Brocks, J. van den Brink, and P. J. Kelly, Phys. Rev. B **78**, 195419 (2008).
[11] M. Ezawa, Eur. Phys. J. B **67**, 543 (2009).
[12] T. B. Martins, A. J. R. da Silva, R. H. Miwa, and A. Fazzio, Nano Lett. **8**, 2293 (2008).
[13] J. Guo, D. Gunlycke, and C. T. White, Appl. Phys. Lett. **92**, 163109 (2008).
[14] L. V. Keldysh, Sov. Phys. JETP **20**, 1018 (1965); C. Caroli, R. Combescot, P. Nozieres, and D. Saint-James, J. Phys. C **4**, 916 (1971).
[15] H. Kondo, H. Kino, J. Nara, T. Ozaki, and T. Ohno, Phys. Rev. B **73**, 235323 (2006).
[16] D. M. Ceperley and B. J. Alder, Phys. Rev. Lett. **45**, 566 (1980); J. P. Perdew and A. Zunger, Phys. Rev. B **23**, 5048 (1981).
[17] P. Hohenberg and W. Kohn, Phys. Rev. **136**, B864 (1964); W. Kohn and L. J. Sham, Phys. Rev. **140**, A1133 (1965).
[18] T. Ozaki, Phys. Rev. B **75**, 035123 (2007).
[19] T. Ozaki, K. Nishio, and H. Kino, Phys. Rev. B **81**, 035116 (2010).
[20] R. Landauer, IBM J. Res. Dev. **1**, 233 (1957); Philos. Mag. **21**, 863 (1970); Y. Meir and N. S. Wingreen, Phys. Rev. Lett. **68**, 2512 (1992).
[21] N. Troullier and J. L. Martins, Phys. Rev. B **43**, 1993 (1991).
[22] T. Ozaki, Phys. Rev. B **67**, 155108 (2003); T. Ozaki and H. Kino, *ibid.* **69**, 195113 (2004).
[23] J. M. Soler, E. Artacho, J. D. Gale, A. Garcia, J. Junquera, P. Ordejon, and D. Sanchez-Portal, J. Phys.: Condens. Matter **14**, 2745 (2002).
[24] T. Ozaki and H. Kino, Phys. Rev. B **72**, 045121 (2005).
[25] http://www.openmx-square.org/.
[26] M. Fujita, K. Wakabayashi, K. Nakada, and K. Kusakabe, J. Phys. Soc. Jpn. **65**, 1920 (1996); S. Okada and A. Oshiyama, Phys. Rev. Lett. **87**, 146803 (2001).
[27] There are four possible spin configurations: (i) the AFM coupling between the edges and the FM junction, (ii) the AFM coupling between the edges and the AFM junction, (iii) the FM coupling between the edges and the FM junction, and (iv) the FM coupling between the edges and the AFM junction. The spin configuration we consider in the paper is the case (iv) which produces spin-polarized band structure as shown in Fig. 3. When the bias voltage is applied to the case (iv), both the channel between the π and π states and that between the π^* and π^* states become available in the energy regime between two chemical potentials, leading to electric current. If the bias voltage is reversed, the two channels become available for the other spin state, which results in the dual spin filter effect. In the case (i), it is clear that such a filter effect does not occur, since the effect of the bias voltage is independent of the spin state. In the case (iii), the bias voltage affects nearly equivalently to each spin state, leading to no spin filter effect. In the case (ii) there is no channel between the π and π states and that between the π^* and π^* states in the energy regime between two chemical potentials. Therefore, the case (ii) also does not exhibit such a spin filter effect. Also, we have confirmed above the statement by the NEGF calculations.
[28] N. Marzari and D. Vanderbilt, Phys. Rev. B **56**, 12847 (1997).
[29] H. Weng, T. Ozaki, and K. Terakura, Phys. Rev. B **79**, 235118 (2009).